Korean J. Chem. Eng., 40(6), 1486-1496 (2023)
DOI: 10.1007/s11814-022-1289-7

pISSN: 0256-1115
eISSN: 1975-7220

One-step solvothermal synthesis of poly(arylene ether nitrile) decorated magnetic composite for methylene blue adsorption from aqueous solution

Xuefei Zhou*, Wei Miao*,†, Wenxi Cheng*, Haowei Lin*, Jinling Li*, Hongjuan Zheng*, Qiaohuan Cheng*, Renjie Wang*, Chenxue Yao*, and Xiaobo Liu,†**

*School of Materials Science and Engineering, Henan University of Technology, Zhengzhou, 450001, China
**Research Branch of Advanced Functional Materials, School of Materials and Energy, University of Electronic Science and Technology of China, Chengdu, 610054, China
(*Received 16 June 2022 • Revised 12 September 2022 • Accepted 13 September 2022*)

Abstract−A series of poly(arylene ether nitrile) containing versatile carboxyl and sulfonic groups (CSPEN) were magnetically functionalized by ferroferric oxide (Fe_3O_4), and the obtained magnetic adsorbents (Fe_3O_4/CSPEN) were used to remove methylene blue (MB) dye from aqueous solution. The systematical characterizations that including scanning electron microscope (SEM), X-ray powder diffractometer (XRD), X-ray photoelectron spectroscopy (XPS), vibrating sample magnetometer (VSM), Fourier transform infrared (FTIR) certified that the Fe_3O_4/CSPEN possessed versatile functional groups and magnetic separation properties. The batch adsorption studies revealed that the Fe_3O_4/CSPEN not only displayed high selective adsorption ability for cationic MB in the presence of anionic MO, but also exhibited a removal efficiency as high as 98.2%. Besides, the adsorption kinetics and isotherm matched well with pseudo-second-order model and Langmuir model, respectively, and the maximum adsorption capacity of Fe_3O_4/CSPEN for MB was 92.029 mg/g. The FTIR and Brunauer-Emmett-Teller (BET) analyses confirmed that the outstanding adsorption capacity of Fe_3O_4/CSPEN was attributed to their own microporous structure and the electrostatic interaction with MB. Therefore, the modified magnetic adsorbent can be used to selectively remove cationic dye from aqueous solution.

Keywords: Poly(Arylene Ether Nitrile), Fe_3O_4, Solvothermal Method, Adsorption, Methylene Blue

INTRODUCTION

Water resource has always been a precious treasure for the whole ecosystem; however, rapid industrialization is on the way to destroy it by discharging quantities of non-biodegradable contaminants [1,2]. Dyes, as the most widely used compounds in many fields such as textile, paper, leather, printing, etc., are the one of the main water pollutant sources [3]. Since dyes are generally composed of aromatic structures, untreated dye contaminants are hazardous and highly resistant to degradation; moreover, they directly impede sunlight transmission and photosynthesis of aquatic life [4,5]. Faced with a serious environmental crisis caused by dye effluents, numerous methods, including coagulation/flocculation, adsorption, microbial degradation, electrochemical oxidation, membrane filtration and photocatalytic degradation, have been developed to alleviate the environmental stress [6,7]. Compared with most of the above treatments, adsorption is distinguished for its low-cost, high-efficiency and no generation of toxic byproduct [8-10]. Especially, the polymer based micro- and nanomaterial adsorbent has attracted increasing interest for its feasibility to modulate the functional groups and morphology [11]. It was acknowledged that the functional groups on adsorbent were vital for adsorption of targeted dyes via electrostatic interaction, while the increased reactive sites on hierarchical morphology were also beneficial for the dye's adsorption capacity.

Although the polymeric adsorbents in micro- or nanoscale were generally high-efficient in removing dyes effluent, they faced with the same recycling difficulties as all other commonly used adsorbents [12,13]. For traditional adsorbents, the generally used separation techniques like centrifugation and filtration are time-consuming, high cost and even bring in secondary pollution. It is difficult to popularize these adsorbents in disposing large-scale effluent. Fortunately, magnetic based adsorbent can avoid the above defects, for they can be easily separated from wastewater with the assistance of an external magnetic field [14]. Moreover, many researchers have focused on the polymer functionalized magnetic adsorbents, since the specific polymer not only increases the sites for dye adsorption but also prevents the aggregation of adsorbent particles [15,16]. Generally, several steps are required for the fabrication of polymer-based magnetic adsorbents. Dong's group demonstrated a kind of polycarboxylic magnetic polydopamine sub-particle (Fe_3O_4@PDA-COOH) by loading polydopamine (PDA) on the surface of pre-synthesized magnetic particle (Fe_3O_4) and a further modification with mercaptosuccinic acid (MSA), for the adsorption of malachite green (MG) [17]. After these complicated procedures, the final products were usually in a low yield with a certain amount of byproduct. Hence, exploring a facile and effective method for preparing the magnetic adsorbent is still demanded. Sun et al. reported a facile one-step solvothermal strategy to fabricate magnetite/reduced graphene oxide

†To whom correspondence should be addressed.
E-mail: wei_miao@haut.edu.cn, liuxb@uestc.edu.cn

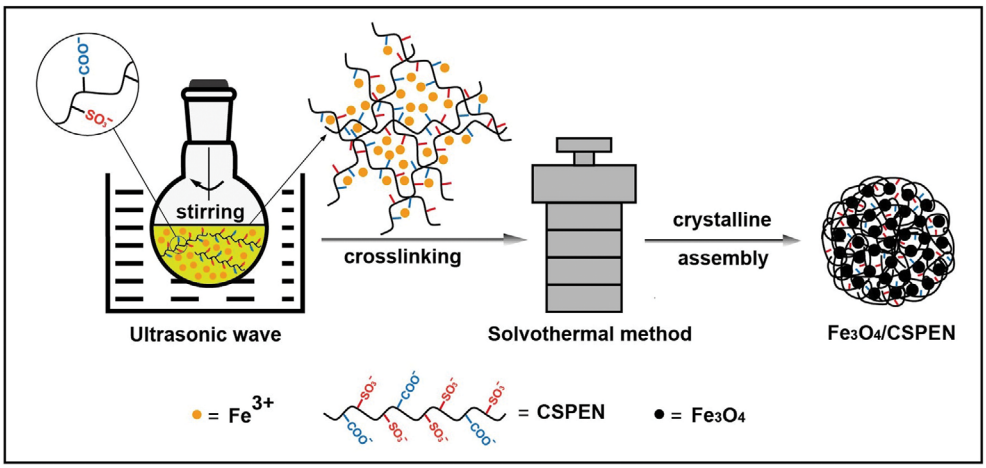

Scheme 1. The preparation route of Fe_3O_4/CSPEN.

(MRGO) nanocomposites based on the coordination of Fe^{3+} with hydroxyl, carboxyl or epoxy groups on GO, which exhibited excellent removal efficiency for rhodamine B and malachite green [18]. Therefore, the functional polymer containing coordination groups is promising in developing an efficient polymeric magnetic adsorbent by the one-step solvothermal method.

Poly(arylene ether nitrile) (PEN) is a kind of high-performance engineering plastic with excellent comprehensive properties, such as high thermostability, corrosion resistance, flame retardancy, strong dimensional stability, processability and designability [19,20]. As an excellent high-performance polymer, the application of PEN has been explored in the field of energy, electronics, aerospace and so on [21]. With the increasing deterioration of the water ecosystem, a novel kind of poly(arylene ether nitrile) containing abundant carboxyl and sulfonic groups (CSPEN) has been prepared and applied in relieving water pollution problem in recent years [22,23]. It was found that surface functional groups aid in the adsorption of CSPEN for dyes and metal ions through specific interaction mechanisms. Especially, it has been verified that the sub-micrometer CSPEN sphere adsorbent was achievable by a Fe^{3+} mediated emulsion self-assembling protocol, which inspired the development of CSPEN based magnetic nanoparticle adsorbent.

Therefore, a kind of CSPEN fabricated magnetic composite (Fe_3O_4/CSPEN) was successfully fabricated and utilized for the elimination of dyestuffs from aqueous solution. The adsorbent was prepared by a facile one-step solvothermal approach along with the cross-linking of Fe^{3+} with CSPEN. Three composite adsorbents with different mass ratio of Fe_3O_4 and CSPEN were subsequently obtained by tuning the CSPEN in solvothermal process. A series of factors in the adsorption process, including ionic type of dyes, dye concentration, contact time, pH, were systematically investigated to reveal the adsorption kinetics, isotherm, and mechanism.

MATERIALS AND METHODS

1. Materials

2,6-Difluorobenzonitrile (DFBN) and potassium hydroquinone sulfonic acid potassium salt (SHQ) were purchased from Sigma Aldrich (Shanghai, China). Potassium carbonate (K_2CO_3, AR), N-methyl pyrrolidone (NMP, AR), toluene, ethanol, dimethyl formamide (DMF), sodium hydroxide (NaOH, AR), phenolphthalein (PP), zinc (Zn), ferric trichloride hexahydrate ($FeCl_3 \cdot 6H_2O$), sodium acetate trihydrate (NaAc), ethylene glycol (EG) and polyethylene glycol (PEG 2000) were supplied from Chengdu Haihong Chemical Co. (Chengdu, China). Methylene blue (MB) and methyl orange (MO) were received from Sinopharm chemical reagent (Shanghai, China). Phenolphthalin (PPL) was synthesized from phenolphthalein (PP), Zn and NaOH [24].

2. Synthesis of CSPEN, Fe_3O_4 and Fe_3O_4/CSPEN

CSPEN was synthesized from DFBN, SHQ and PPL, by the synthesis route shown in Fig. S1. A facile solvothermal method was adopted to prepare Fe_3O_4 and Fe_3O_4/CSPEN, as the preparation route shown in Scheme 1. First, $FeCl_3 \cdot 6H_2O$ (2.7 g) was dispersed in EG (70 mL) under continuous stirring. Then, the CSPEN solution (8 mL) with DMF as solvent and PEG2000 (2 g) was added into the above solution. After NaAc (7.2 g) was gradually added into the solution, the mixture was further stirred accompanied with ultrasonic treatment for 30 min. Then, the solution was sealed in a Teflon-lined stainless-steel autoclave, which was subsequently heated to and maintained at 180 °C for 12 h. The obtained product was washed with ethanol and distilled water for several times, then oven dried at 80 °C. Based on the CSPEN feeding content at 0, 0.03, 0.2 and 0.4 g, the obtained particles were marked as Fe_3O_4, Fe_3O_4/CSPEN-1, Fe_3O_4/CSPEN-2 and Fe_3O_4/CSPEN-3, respectively.

3. Batch Adsorption Experiment

All the adsorption experiments were conducted in a vial placed in a thermostatted water bath. The initial pH of MB solution was adjusted by HCl or NaOH. Typically, the adsorption experiment was carried out by adding 10 mg magnetic particles into 20 mL dye solution at ambient temperature. Under vigorous stirring for a certain time interval, the adsorbent was collected using a magnet and the residual dye concentration in the supernatant was calculated by UV-vis spectra. The initial concentration of MB for analyzing adsorption kinetics was 20 mg/L, and the concentration was in the range of 10 mg/L to 200 mg/L for explaining the adsorption isotherms. The instantaneous adsorption capacity (q_t) and equilib-

rium adsorption capacity (q_e) of MB were calculated according to Eqs. (1) and (2) [25,26]:

$$q_t = \left(\frac{C_o - C_t}{m}\right) \times V \quad (1)$$

$$q_e = \left(\frac{C_o - C_e}{m}\right) \times V \quad (2)$$

where C_o (mg/L) represents the initial concentration of the dye solution, C_e (mg/L) and C_t (mg/L) are the dye concentrations at equilibrium time and given time t. V (mL) and m (mg) represent the volume of dye solution and the mass of adsorbent, respectively.

4. Desorption Study

A desorption study was conducted to evaluate the regeneration property of Fe_3O_4/CSPEN. After reaching adsorption equilibrium, the adsorbent was collected through magnetic separation and subsequently washed several times with ethanol and NaOH (0.1 mol/L) until no dyes were detected in the eluant. The obtained product was re-collected and oven dried at 80 °C, and the re-collected Fe_3O_4/CSPEN was then adopted for the next adsorption of MB (200 mg/L) at ambient temperature.

5. Characterization

The morphologies, crystalline structures, magnetic properties of Fe_3O_4 and Fe_3O_4/CSPEN were detected by scanning electron microscopy (SEM, JMS, 6490LV), X-Ray powder diffractometry (XRD) (Bruker D8 Advance A25X), X-ray photoelectron spectroscopy (XPS, Thermo Scientific Escalab 250Xi) and vibrating sample magnetometer (VSM, Quantum Design, PPMS-9). The thermal gravimetric analysis (TGA) of samples was performed on TA Instruments TGA-Q50. The functional groups of the composite before and after MB adsorption were analyzed by Fourier transform infrared (FTIR) spectrometer (Shimadzu 8400S FTIR). The ultraviolet-visible (UV-Vis) absorption spectra of dye solutions were recorded using a UV-Vis spectrophotometer (TU 1901, Persee). The specific surface areas, total pore volumes and mean pore sizes of samples were characterized by N_2 adsorption-desorption instrument (Quantachrome Instruments, Boynton Beach).

RESULTS AND DISCUSSION

1. Material Characterization

The microstructures and size distributions of pristine Fe_3O_4 and three kinds of Fe_3O_4/CSPEN are displayed in Fig. 1, respectively. The SEM image of pristine Fe_3O_4 in Fig. 1(a) exhibits uniform spheroidal shape with slightly rough surface. As for the Fe_3O_4/CSPEN-1 shown in Fig. 1(b), uniform spheres with rougher surfaces were detected. While the Fe_3O_4/CSPEN-2 and Fe_3O_4/CSPEN-3 morphology in Fig. 1(c) and d displays different morphologies compared with Fe_3O_4/CSPEN-1. Specifically, it was noted that not only the uniformity and particle size of composites obviously decreased,

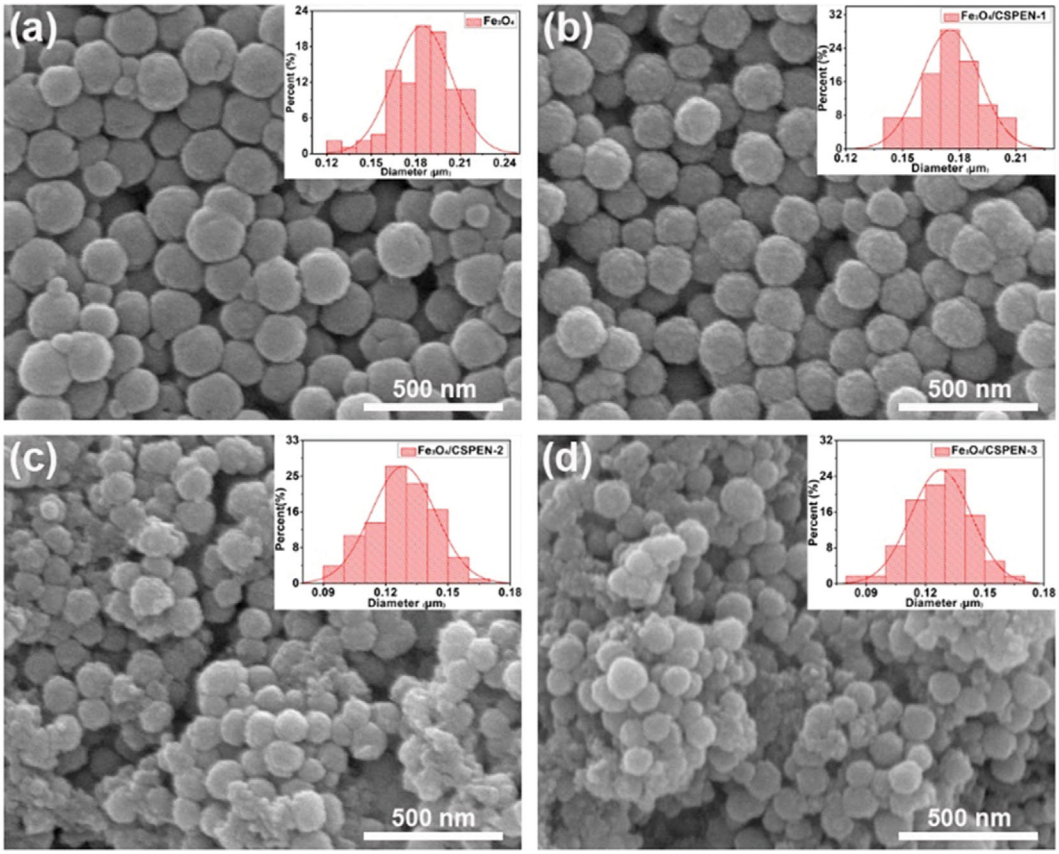

Fig. 1. SEM images and particle size distributions of pristine Fe_3O_4 (a) and Fe_3O_4/CSPEN-1 (b), Fe_3O_4/CSPEN-2 (c), Fe_3O_4/CSPEN-3 (d), respectively.

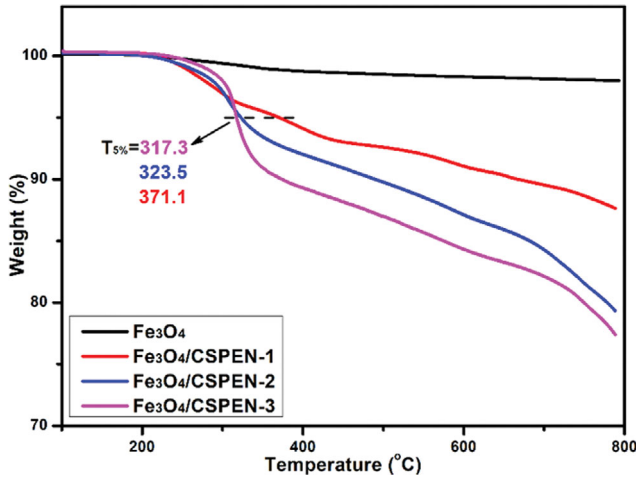

Fig. 2. TGA curves of Fe_3O_4 and Fe_3O_4/CSPEN composites.

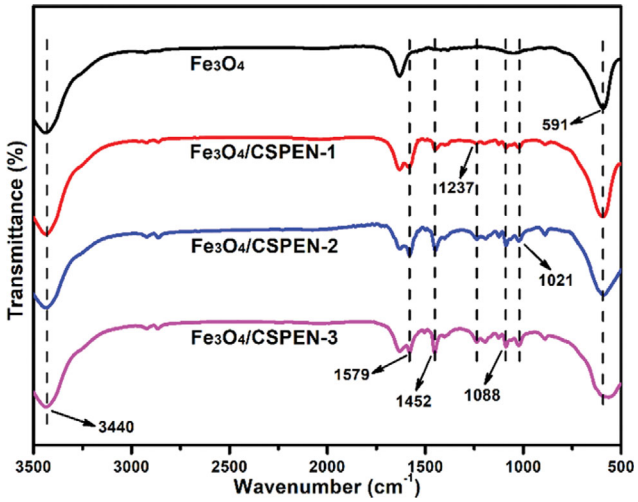

Fig. 3. FTIR spectra of Fe_3O_4 and Fe_3O_4/CSPEN composites.

but also some unregular aggregates that would be ascribed to CSPEN were detected [27]. Moreover, the mean diameter of magnetic particles presented a continuous decrease from 0.185 μm to 0.128 μm, which was attributed to enough CSPEN being supplied abundant crosslinking sites for Fe^{3+} and further limiting the growth of magnetic particles.

Thermal properties of pristine Fe_3O_4 and Fe_3O_4/CSPEN were evaluated by the TA instrument and the results collected as shown in Fig. 2. It was found that no significant weight loss of pristine Fe_3O_4 was detected in the range of 100 °C to 800 °C, which was consistent with the high stability of inorganic particles. Along with the increase of CSPEN dosage, the 5% weight loss temperature ($T_{5\%}$) of Fe_3O_4/CSPEN-1, Fe_3O_4/CSPEN-2, Fe_3O_4/CSPEN-3 was detected at 317.3 °C, 323.5 °C and 371.1 °C, respectively, higher than the $T_{5\%}$ of CSPEN detected in Fig. S2. It indicates that the CSPEN was successfully introduced to the magnetic particles, and the fast weight loss was ascribed to the functional carboxyl and sulfonic groups

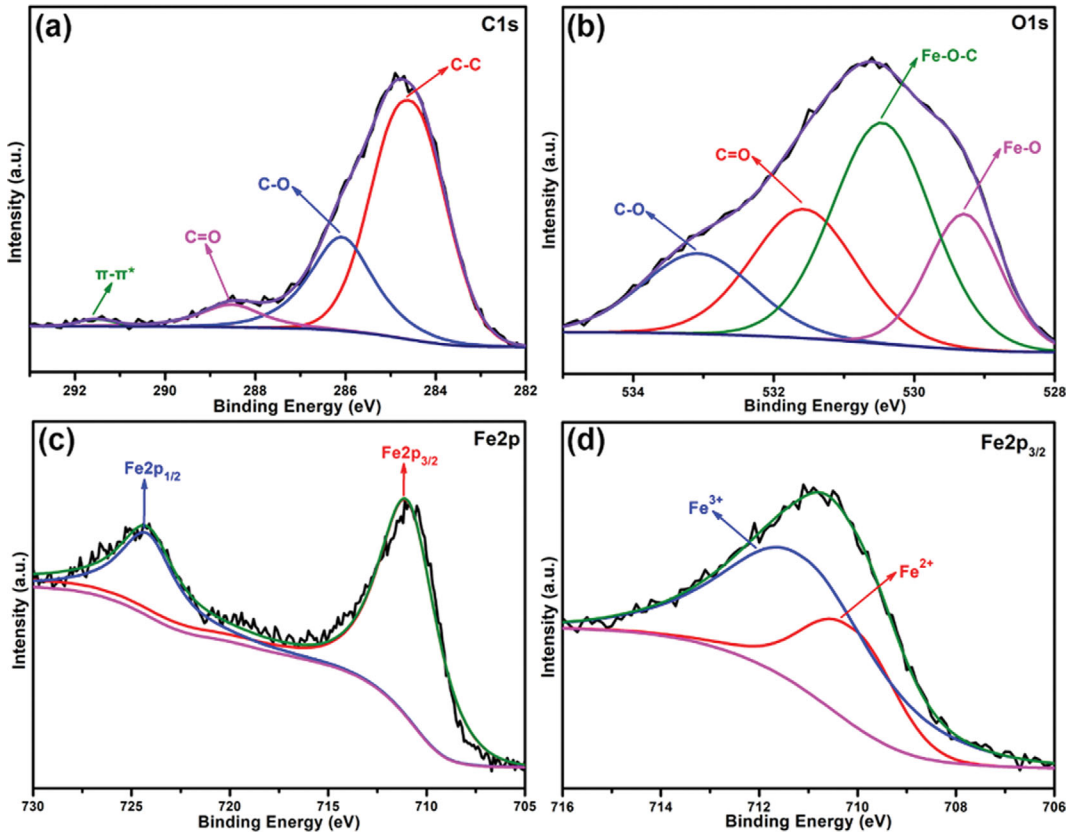

Fig. 4. Peak fitting XPS in C1s (a), O1s (b), Fe2p (c) and deconvolution XPS spectrum of Fe $2p_{3/2}$ (d) for Fe_3O_4/CSPEN.

on CSPEN. Moreover, the increased dosage of CSPEN was believed to be effective for its loading on Fe_3O_4. The mass fraction of CSPEN in Fe_3O_4/CSPEN-1, Fe_3O_4/CSPEN-2 and Fe_3O_4/CSPEN-3 was calculated to be 29.3%, 52.8% and 58.3%, respectively. Besides, the chemical groups of Fe_3O_4 and Fe_3O_4/CSPEN were characterized by Fourier transform infrared spectroscopy.

As shown in Fig. 3, the peaks at around 591 cm^{-1} and 3,440 cm^{-1} were ascribed to the vibrations of Fe-O and O-H bonds of Fe_3O_4, respectively [28]. Compared with the FT-IR spectrum of Fe_3O_4 and CSPEN (Fig. S3), a series of new absorption peaks were detected in the spectra of Fe_3O_4/CSPEN and the increased CSPEN content even contributed to stronger peaks. Among these bands, 1,021 cm^{-1} and 1,237 cm^{-1} were due to the symmetric and asymmetric stretching vibration of Ar-O-Ar. The signals at 1,452 cm^{-1} and 1,579 cm^{-1} belonged to the stretching vibration of C=O group in pendant carboxyl groups, and the 1,088 cm^{-1} was attributed to the stretching vibration of S=O in pendent sulfonic groups, which groups supplied active adsorption sites for the magnetic particles.

Furthermore, the chemical states of Fe_3O_4/CSPEN were characterized by X-ray photoelectron spectra (XPS), as the results show in Fig. 4. The C1s spectra in Fig. 4(a) were fitted into four peaks, which corresponded to C-C (284.8 eV), C-O (286.5 eV), C=O (288.5 eV) and π-π* satellite (291.4 eV) peaks, respectively [29]. The detection of C1s confirmed the successful loading of CSPEN on Fe_3O_4. As for O1s spectra in Fig. 4(b), four strong fitting peaks with binding energy of 529.3 eV, 530.5 eV, 531.6 eV and 533.1 eV were observed. Among these peaks, the peaks at 529.3 eV and 530.5 eV were derived from the Fe-O and Fe-O-C of Fe_3O_4, while the peaks at 531.6 eV and 533.1 eV were ascribed to the C=O and C-O of CSPEN [28]. In Fig. 4(c), the binding energy of 711.1 eV and 724.4 eV belongs to Fe $2p_{3/2}$ and Fe $2p_{1/2}$, which coincide with the values reported for Fe_3O_4 [30]. What is more, the XPS spectrum of Fe $2p_{3/2}$ in Fig. 4(d) was deconvoluted into two peaks at 710.6 eV and 711.7 eV, ascribed to the Fe^{2+} and Fe^{3+} in Fe_3O_4 phase. Based on the mean relative areas of each constituent peak, the Fe^{2+}/Fe^{3+} ratio was calculated to be 0.45. This value was close to the stoichiometric ratio of Fe_3O_4 of 0.5, and the slightly smaller ratio would be ascribed to the fitting error.

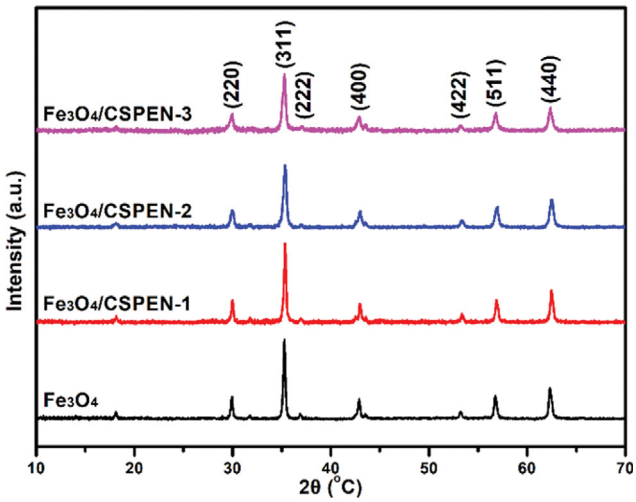

Fig. 5. XRD patterns of Fe_3O_4 and Fe_3O_4/CSPEN.

The crystalline composition and magnetic property of Fe_3O_4 and Fe_3O_4/CSPEN were characterized by X-Ray powder diffractometer and vibrating sample magnetometer, respectively. In Fig. 5, the XRD patterns of all samples present obvious diffraction peaks located at 29.9°, 35.3°, 36.9°, 42.9°, 53.2°, 56.8° and 62.3°, which is consistent with the (220), (311), (222), (400), (422), (511) and (440) planes of standard Fe_3O_4 file (JCPDS no. 019-0629) [31]. Besides, the intensity of all above diffraction peaks presents a decreasing tendency from Fe_3O_4 to Fe_3O_4/CSPEN-3, which would be ascribed to increasingly more CSPEN successfully loaded in Fe_3O_4/CSPEN.

Magnetic hysteresis loop determines the rapid and convenient separation performance of magnetic materials. As the magnetic hysteresis loops show in Fig. 6(a), the magnetic saturation (Ms) intensity of Fe_3O_4, Fe_3O_4/CSPEN-1, Fe_3O_4/CSPEN-2 and Fe_3O_4/CSPEN-3 reached 84.01 emu g^{-1}, 80.65 emu g^{-1}, 73.18 emu g^{-1} and 51.84 emu

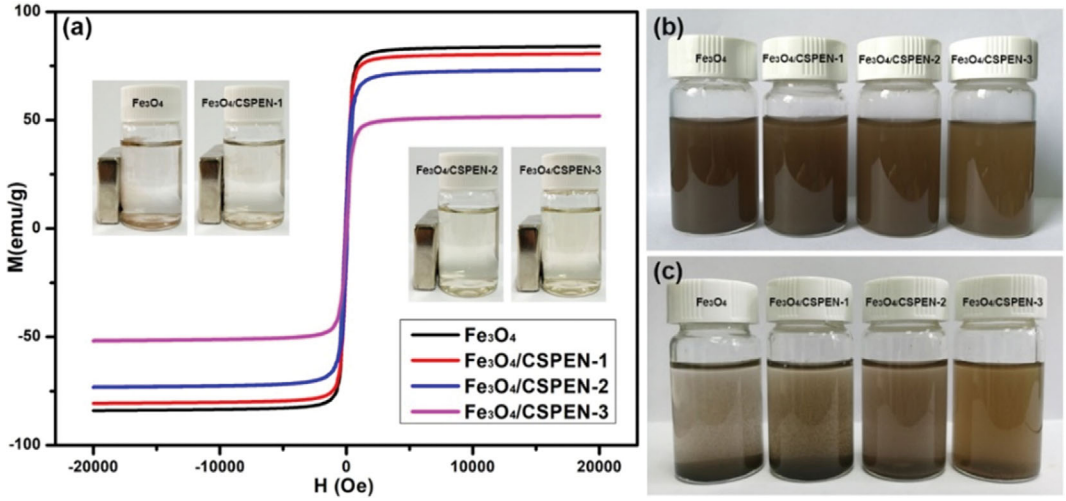

Fig. 6. Magnetic hysteresis loops of Fe_3O_4 and Fe_3O_4/CSPEN, and physical photos of their aqueous solutions in the presence of external magnets (a). Images of magnetic particles before (b) and after (c) standing for 15 min.

g^{-1}, respectively, allowing efficient recollection of the materials with a magnet [32]. The magnetization curves coincided and no hysteresis was observed, implying that they were magnetic [33]. An obvious decrease in magnetic saturation (Ms) intensity indicated the CSPEN was successfully loaded in Fe_3O_4/CSPEN. The physical photos of Fe_3O_4 and Fe_3O_4/CSPEN in aqueous solution with external magnets have been added in Fig. 6(a). These photos indicate that all kinds of magnetic particles can be easily collected in the presence of a magnet, which further certifies their good magnetism and potential high recycling efficiency in dye removal. More-

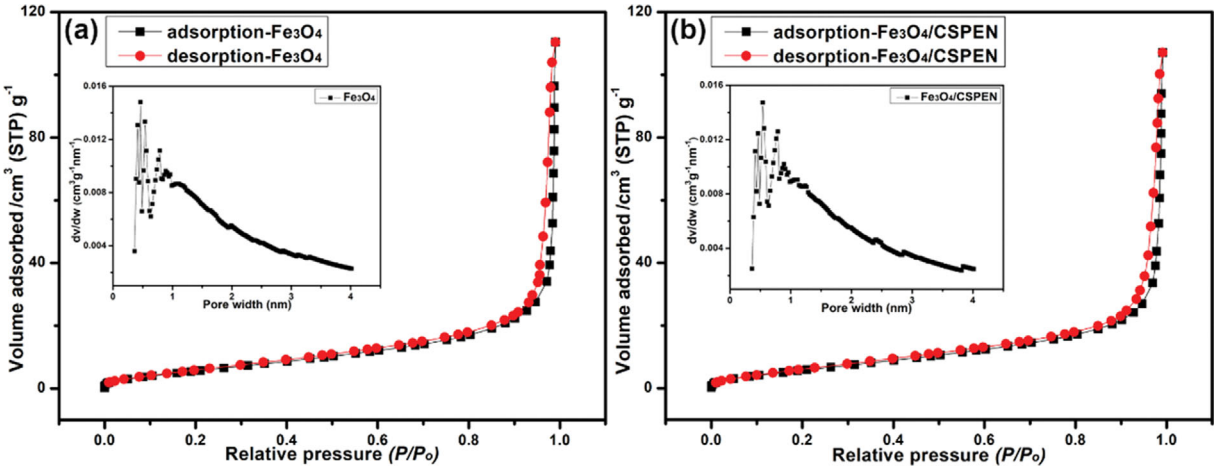

Fig. 7. N_2 adsorption-desorption isotherms and pore diameter distributions of Fe_3O_4 (a) and Fe_3O_4/CSPEN (b) adsorbents.

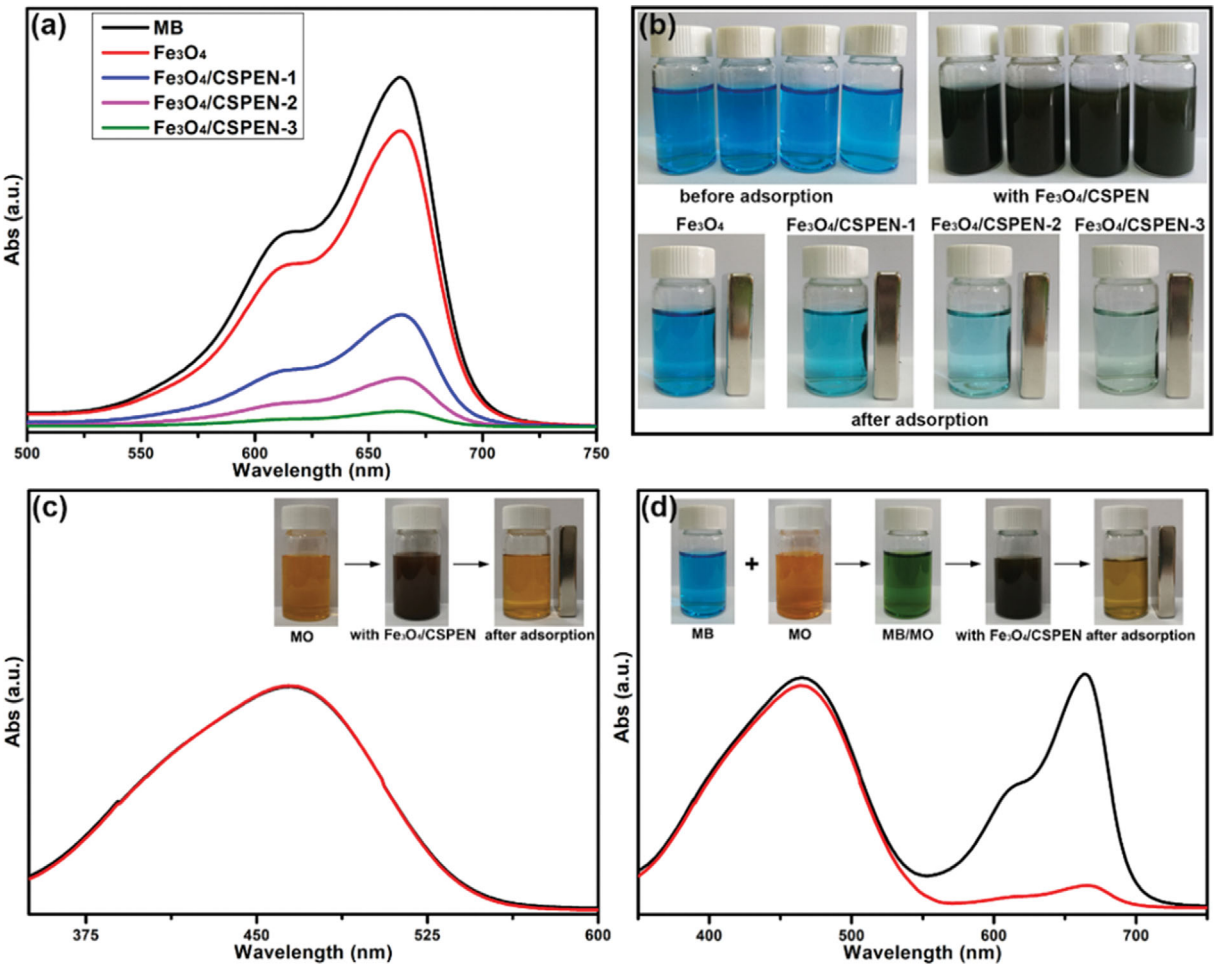

Fig. 8. UV-vis spectra (a) and images of MB (b) in the presence of Fe_3O_4 and Fe_3O_4/CSPEN for 10 min; UV-vis spectra and images of MO (c) and MB/MO mixed solution (d) in the presence of Fe_3O_4/CSPEN for 10 min.

over, the dispersibility of Fe_3O_4/CSPEN in aqueous solution was correspondingly enhanced with the increased loading of CSPEN, as the images show in Fig. 6(b) and (c), which would be beneficial for the approach of water-soluble dyes. These results indicate that the composites possessed outstanding magnetic property and were potential adsorbents for water-soluble dyes.

The physical structure is an important factor to influence the adsorption ability of an adsorbent. As shown in Fig. 7(a) and (b), nitrogen adsorption-desorption measurements were conducted to evaluate the surface properties of Fe_3O_4 and Fe_3O_4/CSPEN adsorbents. According to IUPAC classification, the isotherms of Fe_3O_4 and Fe_3O_4/CSPEN adsorbents can be classified as type IV isotherm with a type H3 hysteresis loop. Based on standard Brunauer-Emmett-Teller (BET) method, the surface area of Fe_3O_4 was enhanced from 25.814 m^2/g to 26.545 m^2/g with the introduction of CSPEN. Additionally, after loading the CSPEN, the pore diameter of magnetic adsorbent slightly increased from 0.46 nm to 0.54 nm and the total pore volumes dramatically decreased from 0.1671 m^3/g to 0.1566 cm^3/g. Consequently, both the microporous structures of Fe_3O_4 and Fe_3O_4/CSPEN adsorbents were beneficial for the adsorption of dyes.

2. Adsorption and Desorption Study

The UV-Vis spectra of cationic dye of MB upon addition of four different magnetic particles in neutral condition are depicted in Fig. 8(a). The characteristic absorption peak of MB at 664 nm slightly decreased in the presence of Fe_3O_4, which was ascribed to the hydroxyl on the surface of Fe_3O_4 [34]. With Fe_3O_4/CSPEN as adsorbent, the adsorption peaks of MB obviously decreased with the increasing loading content of CSPEN in Fe_3O_4. Moreover, all magnetic particles were capable to be separated by magnet, and the color changes of MB in Fig. 8(b) were consistent with the UV-Vis spectra in Fig. 8(a). For comparison, no obvious changes were observed in the absorption spectra of MO with Fe_3O_4/CSPEN as adsorbent, as the image and UV-Vis spectra of MO shows in Fig. 8(c). For further exploring the selective adsorption property of Fe_3O_4/CSPEN, a mixed solution of MB and MO was prepared. As the inset shows in Fig. 8(d), the color of the MB/MO mixed solution changed from blackish green to orange after 10 min, which demonstrated that Fe_3O_4/CSPEN adsorbent had removed MB from the mixture. These results indicate that the as-prepared adsorbent exhibited strong selective adsorption for cationic dye, which has a broad application prospect for the removal of special dye from mixed dyes. Further studies on adsorption properties and adsorption mechanisms were conducted with MB as adsorbate.

The adsorption kinetics isotherms of three composite adsorbents towards MB were investigated. Fig. 9(a) illustrates the effect of ad-

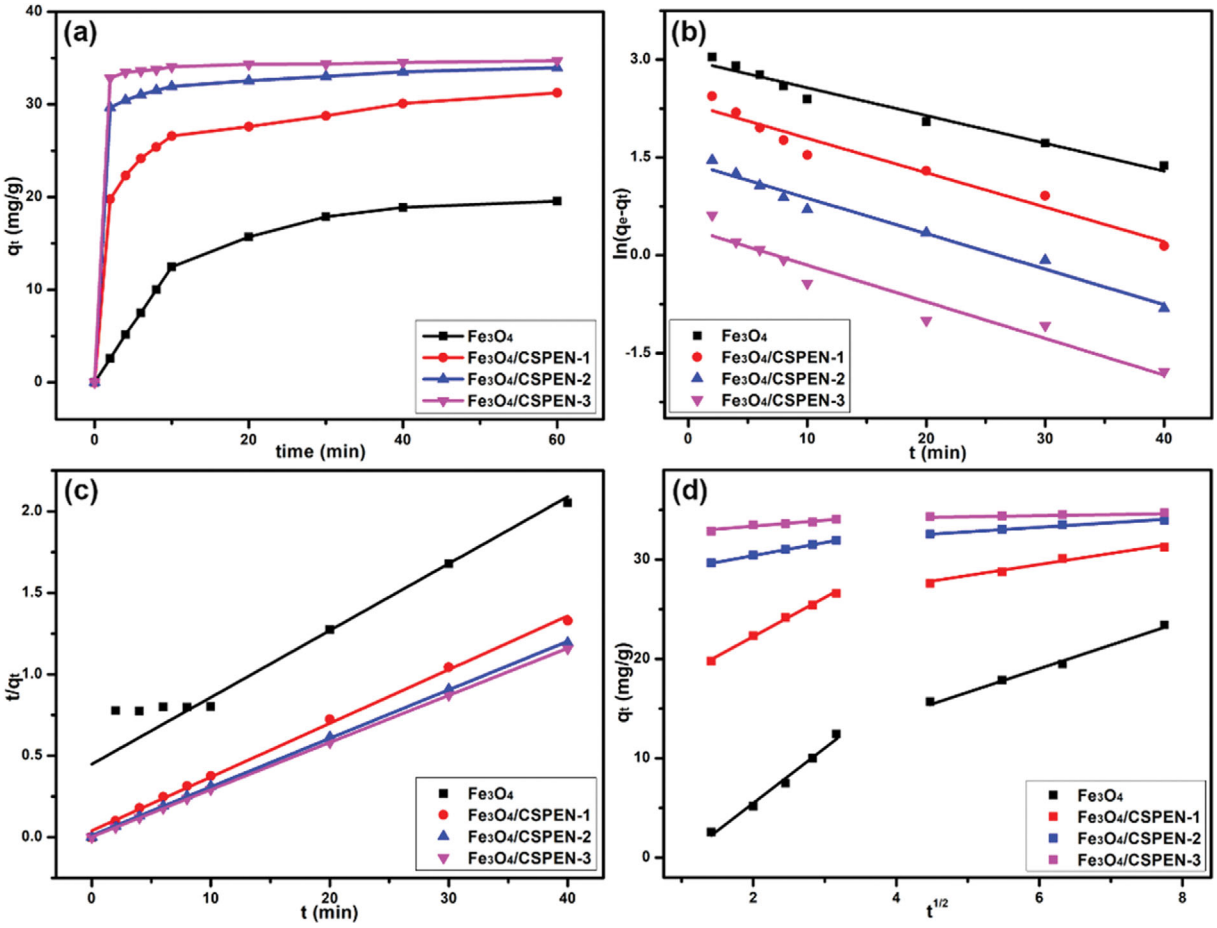

Fig. 9. Effect of contact time on MB adsorption capacity (a), pseudo-first-order model (b), pseudo-second-order model (c) and intraparticle diffusion model (d) for the adsorption of MB onto Fe_3O_4 and Fe_3O_4/CSPEN adsorbents, respectively.

sorption time on the amount of MB adsorbed by the Fe_3O_4 and Fe_3O_4/CSPEN. With the MB concentration of 20 mg/L, the adsorption rate of MB soared in the first 10 min with 63.4%, 85.1%, 93.8% and 98.2% of the ultimate uptake emerging for Fe_3O_4 and Fe_3O_4/CSPEN-1, Fe_3O_4/CSPEN-2 and Fe_3O_4/CSPEN-3. Nevertheless, the adsorption capacity of three Fe_3O_4/CSPEN adsorbents was found conspicuously increased at the initial stage, then slowed until it reached equilibrium. For further exploring the adsorption mechanism and rate-controlling step, three well-known kinetic models--the pseudo-first-order, pseudo-second-order and intraparticle diffusion models--were used to fit the experimental data, which are correspondingly described as Eqs. (3) to (5) [35]:

$$q_t = q_e(1 - e^{-k_1 t}) \tag{3}$$

$$q_t = \frac{k_2 q_e^2 t}{1 + k_2 q_e t} \tag{4}$$

$$q_t = k_p t^{0.5} + C \tag{5}$$

where k_1 (min^{-1}), k_2 (g mg^{-1} min^{-1}) and k_p (mg g^{-1} $min^{-0.5}$) are the rate constants of pseudo-first-order, pseudo-second-order and intraparticle diffusion model, respectively; t (min) is the contact time and C (mg g^{-1}) is a constant related to the adsorption steps. The related simulation figures and parameters were collected and shown in Fig. 9(b) and (c) and Table 1. As for the three Fe_3O_4/CSPEN, the correlation coefficients (R^2) of pseudo-first-order were found in the range of 0.9204 to 0.9752, which were lower than their R^2 of pseudo-second-order ranging from 0.9975 to 0.9999. Moreover, the calculated q_e (cal.) from pseudo-second-order was found to be closer to the experimental q_e (exp.). These results manifested that the chemisorption mechanism dominated the MB removal process by Fe_3O_4/CSPEN, owing to their sharing or exchange of electrons. Besides, the π-π stacking interaction also would be helpful in the adsorption process, as shown in Fig. S4 [22]. By contrast, the adsorption process with Fe_3O_4 as adsorbent fitted well with pseudo-first-order, which implied it belonged to physisorption. From the intra-particle diffusion modelling results in Fig. 9(d), it was found that the fitting straight lines had excellent R^2 values and deviated from the origin, revealing that the intra-particle diffusion process was associated with the uptake of MB by these magnetic adsorbents. Moreover, the first step diffusion would be owing to the diffusion of MB molecules from solution to the surface of magnetic adsorbents, which was called the film diffusion stage. The second step, known as intraparticle diffusion step, was thought to be determined by the surface structure of magnetic adsorbents [36,37]. Furthermore, all the calculated k_{i1} were bigger than k_{i2}, suggesting that the intraparticle diffusion process was a gradual process.

The adsorption equilibrium isotherm was of significance to expound the interaction between adsorbent and organic dyes, which was also competent in evaluating the maximum adsorption capacity of adsorbent to organic dyes. In this work, the two isothermal models of Langmuir and Freundlich were adopted to analyze the adsorption isotherm of Fe_3O_4/CSPEN adsorbent, as shown in Eqs. (6) and (7) [38]:

$$\frac{C_e}{q_e} = \frac{1}{K_L q_m} + \frac{C_e}{q_m} \tag{6}$$

$$\ln q_e = \ln K_F + \frac{1}{n} \ln C_e \tag{7}$$

Moreover, a separation factor (R_L) related to the Langmuir isotherm was adopted to evaluate the feasibility of adsorption process, as shown in Eq. (8):

$$R_L = \frac{1}{1 + K_L C_o} \tag{8}$$

where K_L (L/mg) and q_m (mg/g) represent the Langmuir adsorption equilibrium constant and maximum adsorption capacity, respectively. K_F and n are Freundlich constants. Generally, the Langmuir isotherm model assumes that the adsorbent has a homogeneous surface and the adsorption is considered as a monolayer uptake of adsorbates onto the adsorbent with finite identical active sites [35]. The Freundlich isotherm model is usually applied for analyzing a multilayer adsorption, which assumes an adsorbent with heteroge-

Table 1. The kinetic parameters of adsorption of MB onto magnetic adsorbents

Models	Parameters	Fe_3O_4	Fe_3O_4/CSPEN-1	Fe_3O_4/CSPEN-2	Fe_3O_4/CSPEN-3
Pseudo-first-order	k_1 (min^{-1})	0.0426	0.0528	0.0544	0.0562
	q_e (cal.) (mg g^{-1})	19.976	10.206	4.1417	1.5080
	q_e (exp.) (mg g^{-1})	23.446	31.253	33.958	34.706
	R^2	0.9655	0.9466	0.9752	0.9204
Pseudo-second-order	k_2 (g mg^{-1} min^{-1})	0.0038	0.0270	0.0779	0.2330
	q_e (cal.) (mg g^{-1})	24.372	30.349	33.591	34.578
	q_e (exp.) (mg g^{-1})	23.446	31.253	33.958	34.706
	R^2	0.8786	0.9975	0.9997	0.9999
Intraparticle diffusion	k_{i1} (mg g^{-1} $min^{-0.5}$)	5.6194	3.8919	1.3039	0.6337
	C_1	−5.782	14.424	27.830	32.053
	R_1^2	0.9842	0.9952	0.9997	0.9352
	k_{i2} (mg g^{-1} $min^{-0.5}$)	2.3540	1.1348	0.4359	0.1197
	C_2	4.9896	22.614	30.645	33.768
	R_2^2	0.9893	0.9745	0.9745	0.9167

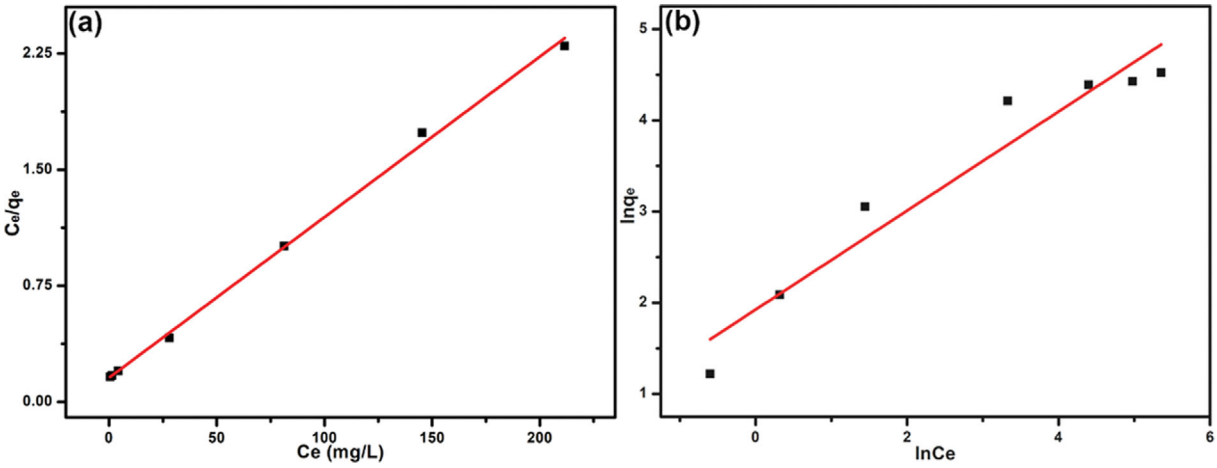

Fig. 10. Langmuir isotherm (a) and Freundlich isotherm (b) for the adsorption of MB onto Fe_3O_4/CSPEN adsorbents.

Table 2. Adsorption isotherm constants for the adsorption of MB onto Fe_3O_4 and Fe_3O_4/CSPEN adsorbents

Isotherm	Parameter	Temperature (K) 298.15
Langmuir	q_m (mg g^{-1})	96.432
	K_L (L mg^{-1})	0.0663
	R^2	0.9989
Freundlich	K_F (L mg^{-1})	6.8562
	n^{-1}	0.5427
	R^2	0.9694

neous energetic distribution. The well-fitted data and parameters of the two models are collected in Fig. 10(a) and (b) and Table 2, which indicates that the Langmuir isotherm model is more qualified to explicate the adsorption isotherm with higher correlation coefficient of 0.9989. Furthermore, the practical value of equilibrium adsorption capacity (92.029 mg/g) was found much closer to the theoretical value (96.432 mg/g) calculated from Langmuir isotherm model. Therefore, it was believed that the adsorption sites on Fe_3O_4/CSPEN were homogeneous, and the adsorption belonged to monolayer adsorption. Besides, the separation factor (R_L) was calculated in the range of 0.0701-0.6031, implying the adsorption of MB onto Fe_3O_4/CSPEN was favorable.

The pH of dye solution influenced the surface charge, ionization degree and dissociation of the functional groups on the surface of adsorbent [39]. With the MB initial concentration of 100 mg/L and the Fe_3O_4/CSPEN dosage of 0.5 g/L, the effect of solution pH on dye adsorption was evaluated with the pH ranging from 2 to 10. As shown in Fig. 11(a), the equilibrium adsorption capacity of Fe_3O_4/CSPEN gradually increased from 67.153 mg/g to 99.292 mg/g along with initial pH of MB solution varying from 2 to 10. It would be ascribed to that the MB solution with higher initial pH was stimulative for the deprotonation of carboxyl and sulfonic groups on CSPEN, which further contributed to the elec-

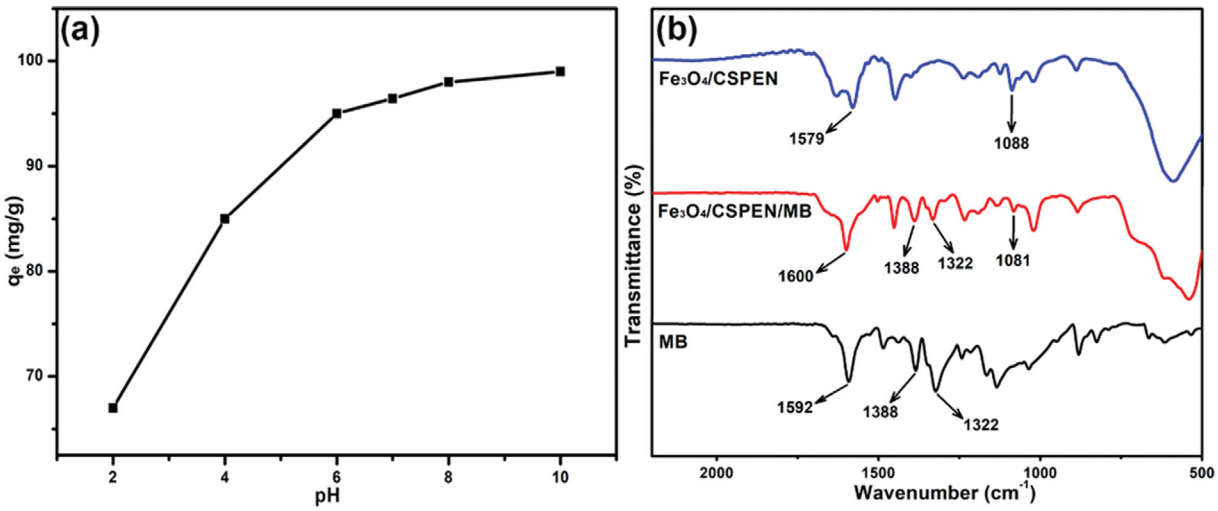

Fig. 11. Effect of pH on the adsorption of MB onto Fe_3O_4/CSPEN (a) and the FTIR spectra of MB, Fe_3O_4/CSPEN and Fe_3O_4/CSPEN/MB (b), respectively.

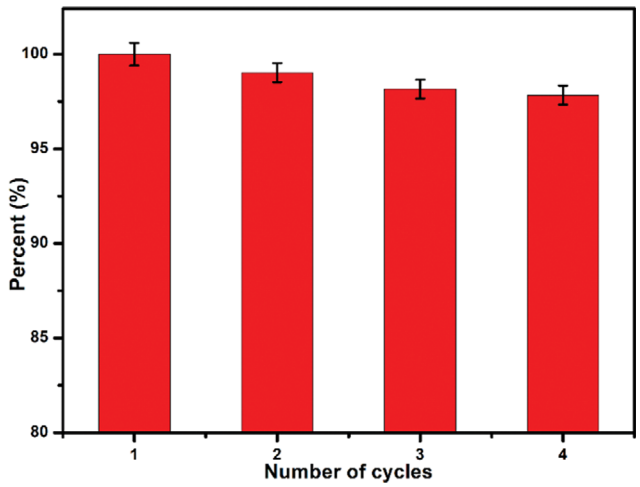

Fig. 12. Regeneration and reuse of Fe_3O_4/CSPEN.

trostatic interaction between anionic CSPEN and cationic MB. The FTIR spectra of Fe_3O_4/CSPEN before and after adsorption are depicted in Fig. 11(b). The peaks located at 1,322 cm^{-1} and 1,388 cm^{-1} were found both in MB and Fe_3O_4/CSPEN/MB, which peaks were, respectively, attributed to the stretching vibration of C-N and the bending vibration of C-H, implying the MB molecules were adsorbed on Fe_3O_4/CSPEN/MB. In addition, a new absorption peak located at 1,600 cm^{-1} was detected, which would be owing to the superposition of the skeleton vibration of benzene rings in MB and the stretching vibration of carboxyl groups in CSPEN, respectively. Also of note is that the absorption band of sulfonic groups in Fe_3O_4/CSPEN moved from 1,088 cm^{-1} to 1,081 cm^{-1} after adsorption, which showed that electrostatic interaction played an important part in MB uptake by Fe_3O_4/CSPEN.

The reusability of adsorbent is a vital factor that determines the effectiveness of adsorption over time. Four cycles of adsorption-desorption were conducted to investigate the stability and reusability of recollected Fe_3O_4/CSPEN. As shown in Fig. 12, the adsorption rate of Fe_3O_4/CSPEN-2 slightly decreased by 2.17% after five successive adsorption-desorption cycles. Moreover, the SEM image of Fe_3O_4/CSPEN-2 maintained morphology, as shown in Fig. S5. Since the Fe_3O_4/CSPEN could be efficiently recycled and reused, it has broad application prospect in the remediation of dyestuffs waste water.

CONCLUSIONS

Fe_3O_4/CSPEN adsorbents were successfully synthesized by the one-step solvothermal strategy for efficient adsorptive removal of dyes from aqueous solution and were effectively characterized by several analytical techniques. The characterization results supported that the Fe_3O_4 was successfully loaded by CSPEN and the obtained Fe_3O_4/CSPEN maintained homogeneous sphere shape. Moreover, the Fe_3O_4/CSPEN exhibited high selective adsorption ability for cationic MB and showed good magnetic recovery capacity. The batch adsorption investigation revealed that the adsorption kinetics isotherms followed pseudo-second-order model, revealing the chemisorption mechanism dominated the MB removal process. Also, the obtained equilibrium data showed a good fit with Langmuir model with a maximum adsorption of 96.432 mg/g, implying monolayer adsorption on the homogeneous adsorption sites on Fe_3O_4/CSPEN. The batch adsorption investigation revealed that the adsorption of MB by Fe_3O_4/CSPEN was pH-dependent, especially the alkaline environment was stimulative for the adsorption. A further study of the adsorption mechanism supported that both electrostatic interaction and the microporous structures of Fe_3O_4/CSPEN contributed to the MB adsorption onto Fe_3O_4/CSPEN. Considering these excellent properties, the developed Fe_3O_4/CSPEN is a promising candidate for effective remediation of dye contaminated water in the near future.

ACKNOWLEDGEMENTS

The authors gratefully acknowledge the Natural Science Foundation of Henan University of Technology (2020BS038) and Higher youth backbone teachers funded in colleges and universities of Henan province in 2019 (grant number 21220028).

DECLARATION OF COMPETING INTEREST

The authors declare that they have no known competing financial interests or personal relationships that could have appeared to influence the work reported in this paper.

SUPPORTING INFORMATION

Additional information as noted in the text. This information is available via the Internet at http://www.springer.com/chemistry/journal/11814.

REFERENCES

1. G. Crini and E. Lichtfouse, *Environ. Chem. Lett.*, **17**, 145 (2018).
2. J. You, L. Wang, Y. Zhao and W. Bao, *J. Clean. Prod.*, **281**, 124668 (2021).
3. D. A. Yaseen and M. Scholz, *Int. J. Environ. Sci. Te.*, **16**, 1193 (2018).
4. V. Katheresan, J. Kansedo and S. Y. Lau, *J. Environ. Chem. Eng.*, **6**, 4676 (2018).
5. F. Mashkoor and A. Nasar, *J. Magn. Magn. Mater.*, **500**, 166408 (2020).
6. Y. Tian, H. Ma and B. Xing, *Appl. Surf. Sci.*, **537**, 147995 (2021).
7. Y. Liu, J. Wang, Y. Wang, H. Zhu, X. Xu, T. Liu and Y. Hu, *Chem. Eng. J.*, **405**, 127051 (2021).
8. C. Feng, P. Ren, M. Huo, Z. Dai, D. Liang, Y. Jin and F. Ren, *Chem. Eng. J.*, **241**, 116369 (2020).
9. M. M. Hassan and C. M. Carr, *Chemosphere*, **265**, 129087 (2021).
10. W. Li, B. Mu and Y. Yang, *Bioresour. Technol.*, **277**, 157 (2019).
11. P. A. Alaba, N. A. Oladoja, Y. M. Sani, O. B. Ayodele, I. Y. Mohammed, S. F. Olupinla and W. M. W. Daud, *J. Environ. Chem. Eng.*, **6**, 1651 (2018).
12. M. I. A. Abdel Maksoud, A. M. Elgarahy, C. Farrell, A. a. H. Al-Muhtaseb, D. W. Rooney and A. I. Osman, *Coordin. Chem. Rev.*, **403**, 213096 (2020).
13. L. Pu, S. Li, Y. Zhang, H. Zhu, W. Fan, P. Ma, W. Dong, Z. Wang

and T. Liu, *J. Mater. Chem. C*, **9**, 2086 (2021).
14. R. Nithya, A. Thirunavukkarasu, A. B. Sathya and R. Sivashankar, *Environ. Chem. Lett.*, **19**, 1275 (2021).
15. J. Qu, M. S. Akindolie, Y. Feng, Z. Jiang, G. Zhang, Q. Jiang, F. Deng, B. Cao and Y. Zhang, *Chem. Eng. J.*, **394**, 124915 (2020).
16. J. Zhang, L. Huang, J. Zheng, J. Xu, A. M. Asiri, H. M. Marwani and M. Zhang, *J. Magn. Magn. Mater.*, **497**, 166011 (2020).
17. X. Pan, G. Zuo, T. Su, S. Cheng, Y. Gu, X. Qi and W. Dong, *Coordin. Chem. RevColloid. Surf. A*, **560**, 106 (2019).
18. H. Sun, L. Cao and L. Lu, *Nano. Res.*, **4**, 550 (2011).
19. M. Feng, C. Li, M. He, Y. Huang and J. Luo, *Ceram. Int.*, **46**, 19181 (2020).
20. L. Wang, X. Liu, C. Liu, X. Zhou, C. Liu, M. Cheng, R. Wei and X. Liu, *Chem. Eng. J.*, **384**, 123231 (2020).
21. M. Feng, M. Chen, J. Qiu, M. He, Y. Huang and J. Lin, *J. Alloy. Compd.*, **856**, 158213 (2021).
22. X. Zhou, M. Xu, L. Wang and X. Liu, *Nanomaterials-Basel*, **9**, 1356 (2019).
23. X. Zhou, P. Zheng, L. Wang and X. Liu, *Polymers-Basel*, **11**, 32 (2018).
24. X. Zhou, L. Wang, X. Liu, M. Xu and X. Liu, *Comps. Part. B-Eng.*, **177**, 107414 (2019).
25. M. Feng, S. Yu, P. Wu, Z. Wang, S. Liu and J. Fu, *Appl. Surf. Sci.*, **542**, 148633 (2021).
26. X. Zhao, X. Wang and T. Lou, *J. Hazard. Mater.*, **403**, 124054 (2021).
27. K. Li, P. Zheng, L. Tong, D. Ren, M. Xu, X. Tang and X. Liu, *Comps. Part. B-Eng.*, **176**, 107202 (2019).
28. Y. Hao, Y. Gao, L. Gao, Y. He, Y. Niu, S. Hussain, R. Gao, L. D. Pfefferle, M. Shahid and S. Wang, *Chem. Eng. J.*, **423**, 129817 (2021).
29. Q. U. Ain, U. Rasheed, M. Yaseen, H. Zhang and Z. Tong, *J. Hazard. Mater.*, **397**, 122758 (2020).
30. H. Guo, Z. Li, L. Xiang, N. Jiang, Y. Zhang, H. Wang and J. Li, *J. Hazard. Mater.*, **403**, 123673 (2021).
31. A. A. Alqadami, M. Naushad, A. L. ZA, M. Alsuhybani and M. Algamdi, *J. Hazard. Mater.*, **389**, 121896 (2020).
32. C. Du, Y. Song, S. Shi, B. Jiang, J. Yang and S. Xiao, *Sci. Total. Environ.*, **711**, 134662 (2020).
33. Y. Liu, Z. Zhu, Q. Cheng, H. Ren, S. Wang, Y. Zhao, J. Li, J. Zhu and L. B. Kong, *J. Magn. Magn. Mater.*, **521**, 167517 (2021).
34. P. T. P. Ryan, D. J. Payne, T. L. Lee and D. A. Duncan, *Phys. Chem. Chem. Phys.*, **24**, 488 (2021).
35. S. Ahmadipouya, M. Heidarian Haris, F. Ahmadijokani, A. Jarahiyan, H. Molavi, F. Matloubi Moghaddam, M. Rezakazemi and M. Arjmand, *J. Mol. Liq.*, **322**, 114910 (2021).
36. R. Foroutan, R. Mohammadi, J. Razeghi and B. Ramavandi, *Algal. Res.*, **40**, 101509 (2019).
37. B. Tanhaei, A. Ayati and M. Sillanpaa, *Int. J. Biol. Macromol.*, **121**, 1126 (2019).
38. S. Joshi, V. K. Garg, N. Kataria and K. Kadirvelu, *Chemosphere*, **236**, 124280 (2019).
39. H. Tang, S. Zhang, T. Huang, F. Cui and B. Xing, *J. Hazard. Mater.*, **395**, 122680 (2020).

Supporting Information

One-step solvothermal synthesis of poly(arylene ether nitrile) decorated magnetic composite for methylene blue adsorption from aqueous solution

Xuefei Zhou*, Wei Miao*,†, Wenxi Cheng*, Haowei Lin*, Jinling Li*, Hongjuan Zheng*, Qiaohuan Cheng*, Renjie Wang*, Chenxue Yao*, and Xiaobo Liu,†**

*School of Materials Science and Engineering, Henan University of Technology, Zhengzhou, 450001, China
**Research Branch of Advanced Functional Materials, School of Materials and Energy, University of Electronic Science and Technology of China, Chengdu, 610054, China
(*Received 16 June 2022 • Revised 12 September 2022 • Accepted 13 September 2022*)

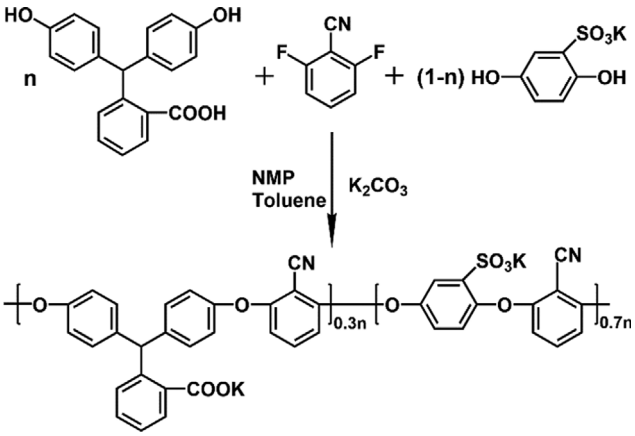

Fig. S1. The synthesis route of CSPEN.

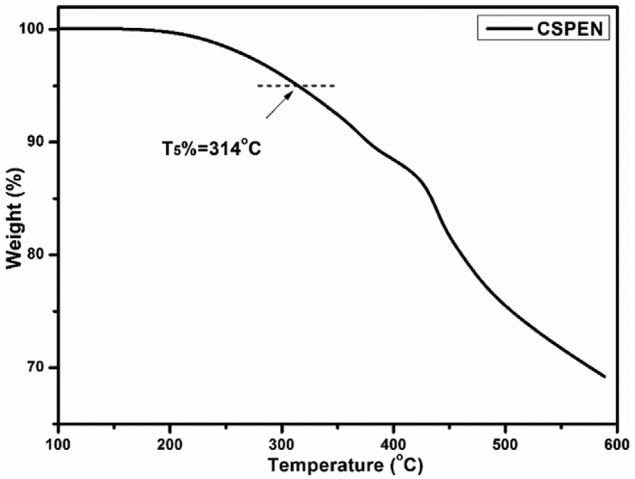

Fig. S2. The TGA curve of CSPEN.

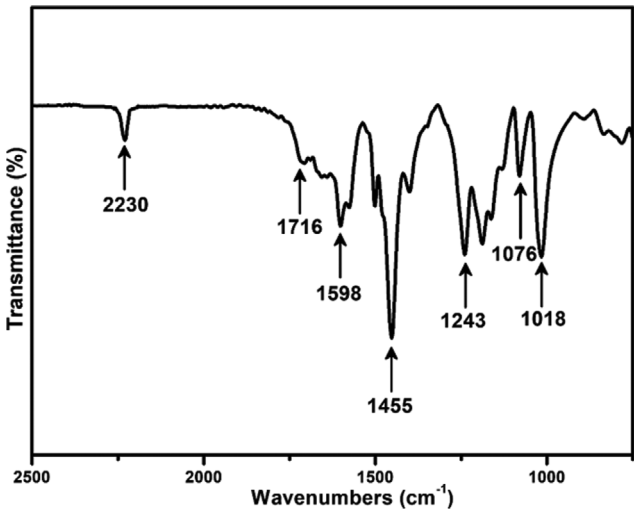

Fig. S3. The FTIR spectrum of CSPEN.

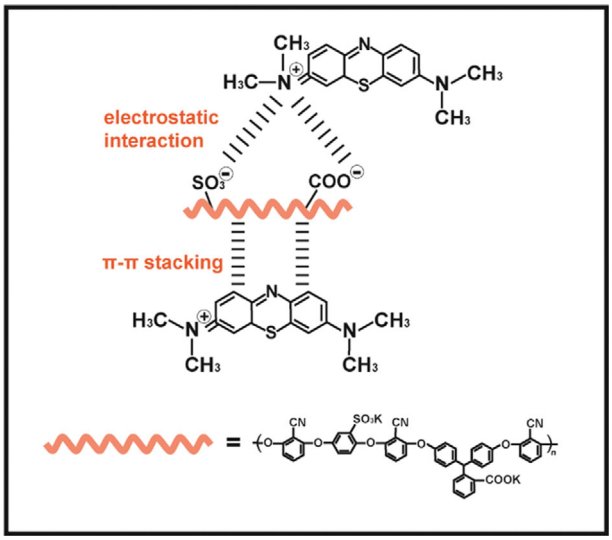

Fig. S4. The supposed mechanism for the adsorption of MB onto Fe_3O_4/CSPEN.

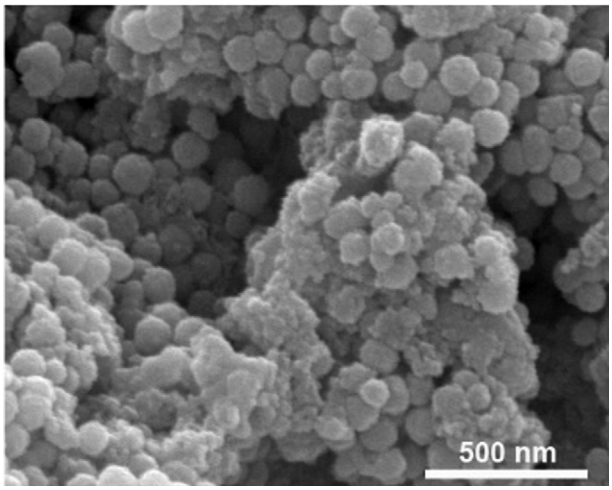

Fig. S5. SEM image of Fe_3O_4/CSPEN-2 after cycling experiment.